Scavenging, cycling and removal fluxes of ^{210}Po and ^{210}Pb at the Bermuda Time-series Study site

G.H. Hong[1,4], M. Baskaran[1*], T.M. Church[2] and M. Conte[3]

*Corresponding Author

1: Department of Geology, Wayne State University, Detroit, MI-48202;
Baskaran@wayne.edu; 313-577-3262
2. School of Marine Science and Policy, University of Delaware, Newark, DE-19716
3: Marine Biological Laboratory, Woods Hole, MA-02543
4: On sabbatical leave from Korea Institute of Ocean Science and Technology, Ansan, South Korea

Deep-Sea Research – II
Special Volume
14 November 2012

Abstract

Quantifying relative affinities of Po and Pb in different populations of marine particulate matter is of great importance in utilizing ^{210}Po as a tracer for carbon cycling. We collected and analyzed water samples for the concentrations of dissolved and total ^{210}Po and ^{210}Pb from the upper 600 m of the water column at Bermuda Time-series Study site (September 1999 to September 2000) to investigate their seasonality of concentrations and their activity ratio (^{210}Po/^{210}Pb activity ratio, AR). Sinking particles collected in sediment traps at depths of 500 m, 1500 m, and 3200 m from the Oceanic Flux Program (OFP) time-series sediment traps were analyzed over a period of 12 months (May 1999 to May 2000). The objective was to compare the deficiencies of ^{210}Po with respect to ^{210}Pb in the water column to that measured in the sediment traps and to assess the relative affinities of Po and Pb with different particle pools.

Inventories of ^{210}Po in the upper 500 m water column varied by a factor of 2, indicating seasonal variations of particulate flux dominated the removal of ^{210}Po. The ^{210}Po/^{210}Pb ARs in the dissolved phase were generally less than the secular equilibrium value (1.0) in the upper 600 m, while were generally greater than 1.0 in the particulate phase, indicating higher removal rates of ^{210}Po relative to ^{210}Pb by particulate matter. The measured fluxes of ^{210}Po and ^{210}Pb in the 500 m, 1500 m, and 3200 m traps increased with depth, while the ^{210}Po/^{210}Pb ARs decreased with depth except from May-August 1999. From the measured fluxes of ^{210}Po and ^{210}Pb at these three traps and the concentrations of ^{210}Po and ^{210}Pb in the water column, this region appears to be a sink for ^{210}Pb which is likely brought-in by lateral advection.

1. Introduction

The $^{210}Po/^{210}Pb$ pair in the ^{222}Rn decay chain can provide wealth of information on rates of diverse oceanic processes at ocean boundaries integrated over time scales of a few days to the mean-life of ^{210}Po (199.7 days). The pair was extensively studied during GEOSECS by several research groups (e.g., Cochran et al., 1983; Chung and Finkel, 1988) in 1970s and the pair was again selected as one of the priority tracers for the GEOTRACES program from 2008 onwards with the mission of assessing their sources, sinks and internal cycling and to characterize the physical, chemical and biological processes that regulate their distribution, in particular across major ocean boundaries (Church et al., 2012). This includes export fluxes of POC, lithogenic and sulfur-group elements from the euphotic zone, rates of remineralization of ^{210}Po and other sulfur-group organic material, residence times and removal rates of Po and Pb and other lithogenic and biogenic proxy elements. For example, the distribution of particulate and dissolved ^{210}Po and ^{210}Pb in surface water has aided to constrain the new production rates (e.g., Sarin, et al., 1994).

The concentration of ^{210}Pb in the surface waters primarily depends temporally and geographically on the varying inputs of atmospheric deposition and removal on to particles, and secondarily on the redistribution by advection and diffusion. Most of the dissolved ^{210}Po in the upper water column is produced during the decay of ^{210}Pb via ^{210}Bi ultimately derived from the atmospheric fallout and it is usually depleted with respect to ^{210}Pb because the $^{210}Po/^{210}Pb$ activity ratio (AR) in the atmospheric deposition (both dry and wet deposition) is usually < 0.1 (e.g., Hussain et al., 1998; Sarin et al., 1999; McNeary and Baskaran, 2007; Church and Sarin, 2008; Baskaran, 2011). Though the global average of $^{210}Po/^{210}Pb$ AR in precipitation and atmospheric aerosols is < 0.1, and most of the ^{210}Po in the upper waters are derived from the decay of dissolved and particulate ^{210}Pb, the areas that are affected by volcanic emissions have high amounts of volcanic-eruption-derived ^{210}Po in the atmosphere (Baskaran, 2011).

Laboratory studies have demonstrated a distinct biological enrichment of ^{210}Po in phytoplankton as enrichment factor is in the order of $^{210}Po >> ^{210}Pb \sim Th > Ra > U$ (Fisher et al., 1983, 1987). The fractionation factor calculated from the distribution of these nuclides in the water column agrees with that reported to be $^{234}Th > ^{210}Po > ^{210}Pb$ (Shannon et al., 1970; Tsunogai and Nozaki, 1971; Kharkar et al., 1976; Heyraud and Cherry, 1979; Cochran et al., 1983; Kadko, 1993). Due to stronger bioaccumulation of Po in organic tissues relative to Pb,

Po is more efficiently recycled during particle remineralization and thus has a longer residence time in the water column than Pb (e.g., Stewart et al., 2005). This implies that organic-rich suspended particles in the upper water column will tend to have higher specific ^{210}Po activity as well as ^{210}Po/^{210}Pb activity ratios. However, in some regions, the specific circulation patterns in a given area can lead to total ^{210}Po/^{210}Pb ratios of about unity, for instance in the center of gyres or as a consequence of upwelling (Nozaki et al., 1976; Thomson and Turekian, 1976; Kadko, 1993; Masqué et al., 2002). The oceanic distribution of ^{210}Po has also direct relevance to global biogeochemical cycling of other sulfur group elements (e.g., S, Se, and Te) and their utility as a tracer for nitrogen fixation (Kim and Church, 2001).

In deep waters below 1000 m, secular equilibrium between ^{210}Po and ^{210}Pb (^{210}Po/^{210}Pb AR ~ 1) was observed in some areas (e.g. North Atlantic: Bacon et al., 1976; South Pacific; Turekian and Nozaki, 1980; Central and Eastern Indian Ocean: Cochran et al., 1983; Indian Ocean: Chung and Finkel, 1988)), however, a large scale deficiency of ^{210}Po with respect to ^{210}Pb (^{210}Po/^{210}Pb AR < 1) has also been reported in various parts of the world ocean (e.g. East China and Philippine Sea: Nozaki et al., 1990; Equatorial Pacific and Bering Sea: Nozaki et al., 1997; Sargasso Sea: Kim and Church, 2001; South China Sea: Chung and Wu, 2005; Church et al., 2012). Sampling and analytical problems with the ^{210}Po/^{210}Pb measurements have been reported in the past. For example, samples collected from 1500 to 4000 m off the coast of Peru showed a pronounced ^{210}Po deficiency (^{210}Po/^{210}Pb <1, Thomson and Turekian, 1976). However, examination of new set of samples from the same area revealed equilibrium (^{210}Po/^{210}Pb ~ 1) and this difference was attributed to the loss of Po onto the walls of sampling bottles due to storage of samples (Turekian and Nozaki, 1980). Mechanistic detail for this deficiency therefore remains elusive up to date.

In this article, we report vertical profiles of dissolved and total (= particulate + dissolved) ^{210}Po and ^{210}Pb concentration and ^{210}Po/^{210}Pb ARs in the upper 600 m at the Bermuda Time-series Study (BATS) site along with their concentrations and ARs in sediment trap samples from 500m, 1500m and 3200m depths collected concurrently by the Oceanic Flux Program (OFP). The primary goal is to understand the cycling of Po and Pb in the upper water column by comparing variations in ^{210}Po and ^{210}Pb concentrations and the ^{210}Po/^{210}Pb ARs in the upper water column with concurrently measured depositional fluxes of ^{210}Po and ^{210}Pb in sediment traps at 500m, 1500m, and 3200m.

2. Materials and Methods

Seawater and sediment trap (500, 1500, and 3200 m) samples were collected at the BATS site ($31^0$40'N, $64^0$10'W), located approximately 75 km southeast of Bermuda in 4500 m water depth. Seawater samples were collected bimonthly from September 1999 to September 2000 from the surface to ~600 m to obtain high-resolution ^{210}Po-^{210}Pb profiles. Concurrent to the radionuclide sampling, other relevant biogeochemical variables including nutrients, productivity (^{14}C-based), and POC were also measured (nutrients and primary productivity data can be found at http://bats.bios.edu/bats_form_prod.html).

Sinking flux material collected by the Oceanic Flux Program (OFP) (Conte et al., 2001; 2003) over the same time period was also analyzed for ^{210}Po and ^{210}Pb. The OFP mooring consists of three Parflux sediment traps (0.5 m^2 surface area) deployed at 500, 1500 and 3200 m and programmed at a nominal two weeks sample integration period. The trap brine is poisoned with ultra-purity mercuric chloride (200 mg/L) to arrest any bacterial activity.

The analytical procedure for the determination of ^{210}Po and ^{210}Pb is given in Kim (2001). Briefly, ~20 liter water samples were collected in collapsible cubitainers and utilized for total ^{210}Po-^{210}Pb measurements. For the dissolved phase, water samples were filtered through 0.45-μm cartridge filter using a small pump (JABSCO). The filtration was completed within an hour of sampling on board in order to minimize the loss of dissolved nuclides by sorption on to the surface of the sampling bottles, and possible alteration of the particles, such as particle settling and break-down, although particle integrity was not verified separately. The filtered and unfiltered (or total; here onwards 'total' and 'unfiltered' are synonymously used) water samples were acidified to pH < 1, and chemical yield tracers (~ 2 dpm of ^{209}Po, 5 mg of Pb) and Fe^{3+} carriers were added. The spikes and carriers were allowed to equilibrate and the pH was adjusted to ~7 using NH_4OH. After settling for ~4-5 hours, the supernatant was siphoned off and the residual mixture was centrifuged. The precipitate was dissolved in 0.5 M HCl. To this solution, 200 mg of ascorbic acid was added to reduce Fe^{3+} to Fe^{2+}. After plating, the solution was dried and taken in 9M HCl. This solution was passed through a 9M HCl anion-exchange resin column to quantitatively separate the Pb from the Po. An aliquot of the separated solution was utilized to measure stable Pb for the chemical yield of Pb (Baskaran et al., 2009). The *in-situ* ^{210}Po was processed within two weeks after sample collection. The plated solution was stored for 1-2 years and again ^{210}Po was re-plated to assay the *in-situ* ^{210}Pb. The in-growth (in-growth factor for the determination of ^{210}Pb from the as-

say of in-grown ^{210}Po, and contribution of ^{210}Po from the decay of ^{210}Pb from the time of collection to first plating) and decay corrections for ^{210}Po and ^{210}Pb were appropriately applied, as detailed in Baskaran et al. (2012, in review). An aliquot of the sediment trap material was digested with conc. HF-HNO_3-HCl with the addition of ~ 2 dpm of ^{209}Po and 5 mg of stable Pb. The digested solution was eventually converted to HCl medium and the pH was adjusted to ~2 using NH_4OH and subsequently plated on to Ag disks, and the rest of the procedure is the same as outlined above. All the analyses of the samples were completed by 2002. Particulate ^{210}Po and ^{210}Pb concentrations were calculated by subtracting the filtered sample activity concentrations from their corresponding unfiltered sample activity concentrations and their measurement errors were propagated.

3. Results and Discussion

3.1 Dissolved and total ^{210}Po and ^{210}Pb in the water column:

The vertical profiles of dissolved and unfiltered (total) ^{210}Po and ^{210}Pb concentrations are plotted in Fig. 1 and the data are given in Appendix-I. Water column concentrations of dissolved ^{210}Po and ^{210}Pb varied seasonally. Total ^{210}Po concentrations were generally higher in the upper 100 m than in deeper waters (100 – 600 m). Concentrations of dissolved and total ^{210}Po and ^{210}Pb in the upper 100m were highest during December (average values for dissolved ^{210}Po: 12.2 dpm/100L in December; 8.4, 7.2, 7.1. and 5.0 dpm/100L in September, January, March and May, respectively) (Appendix-I). Concentrations of dissolved ^{210}Po at a particular depth only varied by a factor of ~2 over the sampling period (e.g., between 6.0 dpm/100L and 12.2 dpm/100L at 50 m layer), while the corresponding ^{210}Pb concentrations varied by less than 10% (e.g., between 17.4 dpm/100L and 19.0 dpm/100L), indicating that the higher ^{210}Po variability is due to variations in biogenic activity which preferentially affects the Po activity. Total ^{210}Pb activity in the upper 100 m from January to May remained constant between 19.2 and 19.8 dpm/100L, indicating relatively uniform atmospheric depositional input of ^{210}Pb and similar removal rates on to particulate matter. The distinctly higher ^{210}Pb concentration in September 2000 is attributed to higher depositional flux due to higher amounts of precipitation and possibly higher atmospheric dust input during the summer time.

The fraction of particulate ^{210}Po was significantly higher than that of ^{210}Pb (Fig. 1, Appendix-I). The fraction of particulate ^{210}Po varied widely, between 5 and 63%, with generally higher percentage in the upper 150m and lower percentage below. The fraction of partic-

ulate ^{210}Pb was lower than that of ^{210}Po and exhibited less than 30%. The high fraction of particulate ^{210}Pb in May was attributed to higher seasonal dust input.

Seasonal inventories of ^{210}Po and ^{210}Pb in the upper 500 m water column for each sampling period varied by factor of ~2 for ^{210}Po, from 2.4 x 10^4 to 4.5 x 10^4 dpm m^{-2} for dissolved ^{210}Po and 8.0 x 10^4 to 10.6 x 10^4 dpm m^{-2} for dissolved Pb, with the highest ^{210}Po values found in December (Table 1). The particulate ^{210}Po inventory was a factor of two larger than that of ^{210}Pb. Large variations in the inventories of ^{210}Po are likely due to seasonal variations in the biogenic particulate matter and its effect on the scavenging of Po. The water column inventories of ^{210}Po (both filtered and unfiltered) correlated with ^{210}Pb negatively (figure not shown); however, the inventories of ^{210}Po and ^{210}Pb correlated with the POC inventories in the upper 500 m, although the data points are very limited (Table 1).

The ^{210}Po/^{210}Pb ARs in the upper 600 m varied between 0.18 and 0.44 in the dissolved phase and 0.17 to 0.71 for the total (Fig. 2). The mean ^{210}Po/^{210}Pb AR was always higher in the total samples compared to the dissolved phase samples and this is attributed to higher ^{210}Po/^{210}Pb ARs in the particulate matter, generally with values >1.0 (Fig. 2). The mean ^{210}Po/^{210}Pb AR for the total samples was higher in January (0.51) and March (0.55) than in May (0.39) and September (0.36). The ^{210}Po/^{210}Pb AR for the upper 500 m (based on the inventories of these nuclides) varied between 0.27 and 0.37 in the dissolved phase and between 0.29 and 0.51 in the total sample (Table 1). The estimated AR for the particulate fraction varied between 0.2 and 10.7 (Appendix-I), similar to the earlier results reported by Kim and Church (2001), Buesseler et al. (2008), and Stewart et al. (2010). The subsurface maximum $^{210}Po_p$/$^{210}Pb_p$ AR was found at 200 m and this is likely due to re-adsorption of Po onto the biogenic particulate matter (Fig. 2c). The steep gradient in $^{210}Po_p$ in the upper 200 m is attributed to the remineralization of biogenic particulate matter and subsequent release of ^{210}Po to the water column.

High concentration of ^{210}Pb in the upper ~ 100 m has been widely reported in literature and is attributed to atmospheric depositional input. In the present study area, the atmospheric depositional input of ^{210}Pb is generally derived from the North American terrestrial material in the winter, as inferred from the atmospheric deposition of stable lead (Veron et al., 1993), and from North Africa (Sahara) in the summer (Kim, et al., 1999); it also could be due to differences in the scavenging intensity of ^{210}Pb from the water column. Higher concentrations of ^{210}Pb in aerosols at Bermuda during summer/fall and lower values during win-

ter/spring have been reported (Hartman, 1987) and thus it is likely that the depositional fluxes are also higher during these seasons. The highest concentrations in the upper 100 m was found in December and this is likely due to higher depositional fluxes during fall where the highest amount of precipitation is also reported (in October; http://www.bermuda-online.org/climateweather.htm). Higher concentrations of ^{210}Po and ^{210}Pb in September and December (Fig.1) could be attributed to higher inputs of Saharan dust during the summer months (Prospero, 1996). The surface depletion of ^{210}Po relative to ^{210}Pb is also attributed to lower ^{210}Po/^{210}Pb ARs in the precipitation as well as in the aerosols deposited onto the sea surface. Although the expected ^{210}Po/^{210}Pb ARs in the original soils and Saharan dust to be ~1.0, this ratio could be significantly altered during the transit due to addition of ^{210}Pb from the aerosols that contain ^{210}Po/^{210}Pb ARs < 0.1. It has been also reported that the atmospheric input of ^{210}Pb to the Atlantic Ocean including the Sargasso Sea is roughly a factor of two or larger than that for the whole of the Pacific Ocean (Cochran et al., 1990).

3.2. Fluxes of particulate ^{210}Po and ^{210}Pb at 500 m, 1500 m and 3200 m depth:

Temporal variation of settling fluxes of particulate ^{210}Po, ^{210}Pb and ^{210}Po/^{210}Pb AR at 500, 1500, and 3200 m depths from May 1999-May 2000 are shown in Fig. 3. The average fluxes of mass, aluminum, calcium carbonate and organic carbon along with settling fluxes of ^{210}Po and ^{210}Pb at 500, 1500, and 3200m depths are also summarized in Fig. 4.

The average activities of ^{210}Po and ^{210}Pb in the 500 m trap with their standard deviation were found to be 265 ± 180 and 543 ± 400 dpm/g and their settling fluxes were found to be 5.5 ± 4.8 and 10.0 ± 9.4 dpm m^{-2} d^{-1}, respectively (Appendix-II). These ^{210}Po values are approximately an order of magnitude lower than that observed at 150 m depth in the region (109 ± 40 dpm ^{210}Po m^{-2} d^{-1}, Stewart et al., 2010; 67 ± 21 dpm ^{210}Po m^{-2} d^{-1}, Buesseler et al., 2008), and indicate that >90% of the ^{210}Po in the sinking particulate matter is remineralized between 150 m and 500 m. At 500 m depth, there is a strong correlation between fluxes of POC and ^{210}Po (R=0.83, P >0.001), mass flux and ^{210}Po flux (R=0.54, P>0.05), and mass flux and ^{210}Pb flux (R=0.63. P>0.05). The ^{210}Po and ^{210}Pb fluxes at 500 m depth varied by an order of magnitude over the study period and they exhibited minimum fluxes during the winter months when mass fluxes were low. Peak fluxes were observed in July and August 1999 (Appendix-II). The ^{210}Po/^{210}Pb AR of the trap material at 500 m varied from 0.2 to 2.3 with an average value of 0.7 ± 0.5 (calculated from data given in Appendix-II). The $(^{210}Po/^{210}Pb)_p$

AR in the coastal and shelf areas where particle concentrations are high, the $^{210}Po/^{210}Pb$ activity ratio is generally < 1.0. For example, activity ratios of 1.3 and 1.3-2.4 were reported in the North Atlantic and Pacific Ocean, respectively (Brewer et al., 1980; Harada and Tsunogai, 1986). They were found to be 0.45 in Santa Barbara Basin (162-377 m depth, Moore et al., 1981) and 0.2-1.4 with in Santa Monica Basin (100-850 m; Huh et al., 1990), where the particle concentrations and fluxes are significantly higher.

The sinking fluxes of particulate ^{210}Po and ^{210}Pb at 1500 m depth varied between 8.2 and 14.8 dpm m^{-2} d^{-1} (mean: 10.6 ± 3.0 dpm m^{-2} d^{-1}) and 0.7 and 49.2 dpm m^{-2} d^{-1} (mean: 13.2± 13.7 dpm m^{-2} d^{-1}), respectively (Fig. 4, Appendix-II). The ^{210}Po flux varied by less than a factor of 2; however, ^{210}Pb activity varied by an order of magnitude during the deployment period of May–December 1999. Lower variability of ^{210}Po is attributed to remineralization. The sinking flux of ^{210}Po at 1500 m was higher than that at 500 m by a factor ~2. The ^{210}Pb flux was generally lower in May through July and higher from September through December. The $^{210}Po/^{210}Pb$ AR of the trap material at 1500 m depth varied from 0.3 to 14.8, with a mean value of 3.4 (Appendix-II). The $^{210}Po/^{210}Pb$ ARs of less than unity (0.8-1.0) was also found at 1000 m and 2000 m depths in the East Sea (Sea of Japan), a marginal sea, during spring when terrestrial particulate matter input is large (Hong et al., 2008). There was a significant correlation between Al and ^{210}Pb flux at 1500 m ($R=0.66$, $P>0.05$), but there was no correlation between Al and Po. There was no significant correlation between POC and ^{210}Po or ^{210}Pb in the 1500 m trap samples (Fig.5 c and d), probably due to sudden change in particle composition (e.g., increase in carbonate and aluminum (terrigenous) containing particles) and changes in the nature of POC.

The average activities of ^{210}Po and ^{210}Pb in sinking particulate matter at 3200 m was 399 ± 185 and 1017± 418 dpm g^{-1}, respectively. These values can be compared to 327 to 980 dpm ^{210}Po g^{-1} and 131 to 391 ^{210}Pb g^{-1}, with a factor of 3 inter-annual variation at one site (32°05'N, 64°15'W) reported by Bacon et al. (1985). The sinking fluxes of particulate ^{210}Po and ^{210}Pb varied between 1.4 and 32.6 dpm m^{-2} d^{-1}(mean: 15.3± 8.9 dpm m^{-2} d^{-1}) and 14.4 and 53.0 dpm m^{-2} d^{-1} (mean:28.5± 10.8 dpm m^{-2} d^{-1}), respectively (Fig. 4). Sinking fluxes of particulate ^{210}Po and ^{210}Pb from an earlier study were reported to be 31.0± 12.0 and 12.2 ± 3.7 dpm m^{-2} d^{-1}, respectively (Bacon et al., 1985). Our data reported in this study falls in the lower end for ^{210}Po, however, it is larger as much as a factor of three compared to that in 1980-81 period (Bacon et al., 1985), due to probably lateral transport of inorganic particles.

The flux measurement reported here are consistent with the range observed in the atmospheric input of ^{210}Pb at Bermuda of 11.2-18.9 dpm m^{-2} d^{-1}, which depends upon the variation of rainfall and origin of air masses descending to Bermuda Island (Turekian et al., 1983; Kim et al., 1999; Cochran et al., 1990). Our values can also be compared to other published values from deep water traps in this region. The settling fluxes of ^{210}Po and ^{210}Pb were reported to be 2.19 ^{210}Po dpm m^{-2} d^{-1} and 1.64 ^{210}Pb dpm m^{-2} d^{-1} at 1000 m, and 18.63 ^{210}Po dpm m^{-2} d^{-1} and 10.1 ^{210}Pb dpm m^{-2} d^{-1} at 4000 m, respectively, in PARFLUX S site (Brewer et al., 1980). The ^{210}Po/^{210}Pb AR of 2.5± 0.3 in 1978-81 periods (Bacon et al., 1985) was significantly higher than 0.5± 0.5 reported in this 1999-2000 study period. A similar depletion of ^{210}Po with respect to ^{210}Pb in the water column in the same region was reported by Kim (2001). There is a significant correlation between ^{210}Po flux and mass flux (R=0.87, P>0.001) and ^{210}Po flux and POC flux (R=0.86, P>0.001).

3.3 Residence Time of ^{210}Po and ^{210}Pb:

Using a simple box model, the scavenging residence times of ^{210}Po (τ_{Po}) with respect to removal onto suspended particulate matter for the upper 400 m may be calculated using the equation (1) given below. This calculation assumes that there is no significant net advection and diffusion fluxes on time scales (months) comparable to the mean-life of ^{210}Po. The scavenging residence time of ^{210}Po is calculated as follows:

$$\tau_{Po} = [I_{AR}/(1-I_{AR})] \times \tau \qquad (1)$$

where I_{AR} is the ^{210}Po/^{210}Pb activity ratio in the upper 400 m and τ is the mean-life of ^{210}Po (199 days). The calculated residence times varied between 67 and 118 days for dissolved phase and 106 to 250 days for total (=dissolved and particulate), with the longest residence time in March and shortest residence time in September. This implies rapid net removal in September and less in March to deeper waters. This is consistent with the reportedly preferred partitioning during late summer by N fixing cyano-bacteria (Kim and Church, 2001). This calculation also assumes that the particle composition has remained constant throughout the seasons and its variation did not play any major role on the removal of particle-reactive radionuclides. However different magnitude of bulk particle flux and seasonal fluxes of biogenic particles (silica, carbonate, and sulfate) indeed do play a role in their residence time (described below).

306 *3.4 Partitioning of ^{210}Po and ^{210}Pb:*

307

308 The fractionation factor ($F_{Po/Pb}$) is defined as the ratio of the distribution coefficient

309 (K_d) of ^{210}Po (K_d^{Po}) to that of ^{210}Pb (K_d^{Pb}).

310

311 — (2)

312 — (3)

313 — — (4)

314 where C_p is the concentration of suspended particulate matter (μg/L), Po_d and Pb_d are the

315 concentrations of dissolved ^{210}Po and ^{210}Pb, respectively and Po_p and Pb_p are the concentra-

316 tions of particulate ^{210}Po and ^{210}Pb, respectively. The fractionation factors varied between

317 0.20 and 82 in the 26 samples for which both ^{210}Po and ^{210}Pb data are available (Appendix-A;

318 the negative values are omitted). The rather large variability may stem from the high variabil-

319 ity in particle composition, such as organic matter, calcium carbonate, opal and lithogenic

320 matter. In only 5 out of 26 samples, the $F_{Po/Pb} < 1$ (at 200m, 300m, 400m in Sept., 2000; 400m

321 in May 2000 and 120m in Jan. 2000, Appendix-A), indicating higher affinity of ^{210}Pb com-

322 pared to ^{210}Po, again indicating stronger Po enrichment to particulate matter in most of the

323 samples compared to ^{210}Pb. The $F_{Po/Pb}$ for the integrated depth of 400 m water column can be

324 calculated as follows:

325

326 $F_{Po/Pb} = [(I_{tPo} - I_{dPo})/(I_{tPb} - I_{dPb})] * (I_{dPb}/I_{dPo})$ (5)

327

328 Where I_{tPo}, I_{dPo}, I_{tPb} and I_{dPb} are the inventories of total ^{210}Po, dissolved ^{210}Po, total ^{210}Pb and

329 dissolved ^{210}Pb, respectively. The $F_{Po/Pb}$ values for the upper 400 m varied between 1.5 and

330 5.5, indicating overall enrichment of Po onto particulate matter. This preferential sorption

331 of Po compared to Pb implies that the K_d of Po > K_d of Pb. However, the particulate enrich-

332 ment of Po can be from its assimilation or metabolized like other O-S group elements in or-

333 ganisms, versus that of Pb which is primarily by physiochemical surface adsorption.

334

335 *3.5. Relationship between ^{210}Po and ^{210}Pb removal rates and major carrier phases:*

336 The fluxes of particulate Al and carbonates at 1500m were greater as much as four

and two times than at 500m, while organic carbon flux was only ~ 10% (1500 m) and 30 % (3200 m) as that of at 500 m (Fig. 4, Table 2). Polonium-210 and ^{210}Pb will likely have differential affinities for specific carrier phases such as organic material, calcium carbonate, and opal or lithogenic facies. Thus, variability in ^{210}Po and ^{210}Pb fluxes and activity ratios may possibly be related to compositional variability. We estimated the lithogenic mass from particulate Al, assuming an average crustal Al content of 84,000 ppm for lithogenic material (Taylor and McLennan, 1985), and the mass of biogenic silica by difference (i.e. subtracting lithogenic, organic carbon, calcium carbonate components from the total mass). The estimated opal/$CaCO_3$ ratio at 3200 m depth over this period is 0.21, and is comparable to the overall mean (0.25) reported for the period of 1978-1984 (Conte et al., 2001).

The significant increase in the flux of lithogenic material with depth supports the conclusion that the deep water column at this site is a substantial sink for advected lithogenic material (Huang and Conte 2009). As suggested by Huang and Conte (2009), a likely source of the deep-water scavenged lithogenic component is continental slope sediments that have been advected by the Gulf Stream into eastern North Atlantic gyre. McCave et al. (2001) found significant variations in trace metal concentrations in intermediate depth waters in the northeastern Atlantic indicating intermittent detachment and lateral advection of nepheloid layers into mid-waters. Detailed mineralogical and chemical analyses of suspended particles profiles across a Gulf Stream-Bermuda transect could provide relevant data to test the hypothesis that the lateral advection and deep water scavenging of lithogenic material sourced from continental margin sediments contributes a significant contribution of the deep particle flux in the northern Sargasso Sea.

3.6. *Possible lateral sources of ^{210}Pb to the OFP area:*

We compare our ^{210}Pb fluxes (9.99 dpm cm^{-2} d^{-1} at 500m; 13.2 dpm cm^{-2} d^{-1} at 1500m; and 28.5 dpm cm^{-2} d^{-1} at 3200m) with two adjoining sites: i) another OFP site (31^{0}40’N, 64^{0}10’W) in Nares Abyssal Plain which is northwest of our sampling station; and ii) in the south, the Hatteras Abyssal Plain (32 °48.6"N, 70°44.6'W) (Cochran et al., 1990). Cochran et al. observed that the mean flux of ^{210}Pb increased from 6.0 to14.0 dpm m^{-2} d^{-1} between the 1436 and 4832 m traps at Nares station. This was attributed to the continued uptake of ^{210}Pb on to small particles as they are transferred through the water column by packaging into large particles and subsequent disintegration of the large particles back into small particles at dif-

ferent depths. Bacon et al. (1985) previously reported 9.6 dpm m^{-2} d^{-1} at 3200 m depth south of the current site (32°05'N, 64 ° 15'W), which is much less than the current observation of 28.5 dpm m^{-2} d^{-1}(Fig. 8). Using the published total ^{210}Pb concentration at the Nares and Hatteras sampling stations (Cochran et al, 1990), and our sediment trap measurements yield ^{210}Pb residence time of 29-32 years in the upper 3200 m water column and it falls within the reported values for the North Atlantic (Bacon et al., 1976).

It was observed that the sinking flux of ^{210}Pb measured using sediment trap and ^{210}Pb inventories in the bottom sediments are not sufficient to balance the atmospheric input and *in situ* production in the water column. About 50% of the ^{210}Pb scavenged from the water column at the Nares and Hatteras Abyssal Plains is not sink to the ocean floor locally but is transported out of the area to sink elsewhere in the north due to boundary scavenging (Bacon et al., 1976). They estimated that the scavenging efficiency of ^{210}Pb in the water column is relatively low (< 50%) in the south of about 45 ° N and high (> 50%) in the north of 50 °N in the North Atlantic. The fluxes of particulate ^{210}Pb in sediment trap at 3200m is about three times as that of 500 m and more than twice as that of 1500m trap (Fig. 4). Although the mass flux at 1500m and 3200m remain the same (Fig. 4), higher flux of ^{210}Pb is likely due to lateral inputs. One can estimate spatial scale due to lateral eddy diffusion transport of ^{210}Pb using the relationship between the time scale of diffusion (t), the scale length (Δx) and eddy diffusion coefficient ($D_E \sim 10^5$ cm^2/s),

$\Delta x = \sqrt{(D_E \cdot \tau_E)}$.

Over the mean life of ^{210}Pb of 32.2 yrs, the length scale is ~100 km. Thus, substantial amount of material can be laterally transported to the sampling site.

4. Conclusions

Based on the data presented, we draw the following conclusions: i) there is disequilibrium between dissolved^{210}Po and ^{210}Pb throughout the upper 600 m water column, indicating preferential scavenging of ^{210}Po on monthly time scales; ii) residence times of ^{210}Po in the upper 400 m depth varied seasonally between 67 and118 days for the dissolved phase, which we attribute to differences in the biological cycling; iii) the fractionation factor of Po versus Pb ($F_{Po/Pb}$) integrated over 600 m depth varied between 1.5 and 10.5, again indicating preferential biological sorption of Po over Pb in the upper 600 m water; iv) Fluxes of both ^{210}Po and ^{210}Pb increased with depth and the ^{210}Po/^{210}Pb AR deceased also with depth, although the

fluxes and $^{210}Po/^{210}Pb$ AR were similar between 1500 m and 3200 m depths; v) the $^{210}Po/^{210}Pb$ AR in the deep particle flux at 3200 m depth was generally < 1.0. This depletion can be attributed to scavenging by terrigenous suspended particulate matter that is depleted in ^{210}Po; vi) We did not find any correlation between Al and ^{210}Po in any of the depths, but we found significant correlation between ^{210}Pb and Al as well as ^{210}Po and POC; vii) Our measurements of fluxes of particulate ^{210}Po and ^{210}Pb at 1500 and 3200 m depths appear to be lower in ^{210}Po and higher in ^{210}Pb fluxes at 3200 m depths than the previously reported and could be attributed to variations in the amount of lithogenic and biogenic particulate matter over time; and viii) From the measured fluxes of ^{210}Po and ^{210}Pb at 500 m, 1500 m, and 3200 m traps, it appears that this region is a sink for lithogenic elements and they are likely brought by lateral advection.

Acknowledgements

We thank the two anonymous reviewers for a thorough review of the earlier version of this manuscript. N. Hussain, L. Alleman, C. Hill and A. Bahrou helped us with the analysis of ^{210}Po and ^{210}Pb on these set of samples and their help is appreciated. We also thank the crew of the R/V Weatherbird for their assistance with shipboard sampling. JC Weber of the OFP time-series is acknowledged for his contributions in laboratory analyses of OFP samples. GHH's sabbatical leave was supported by Korea Ocean Research and Development Institute (renamed as Korea Institute of Ocean Science and Technology) (PG47900 and PE98742). The Oceanic Flux Program has been supported since inception by the NSF Chemical Oceanography Program, most recently by grants OCE-0325627/0509602, OCE-0623505 and OCE-0927098. Partial support in writing this manuscript was supported by OCE-0961351 (MB).

References

Bacon, M. P., Huh, C.-A., Fleer, A. P. Deuser, W. G., 1985. Seasonality in the flux of natural radionuclides and plutonium in the deep Sargasso Sea. Deep-Sea Research 32, 273-286.

Bacon, M. P., Belastock, R.A., Tecotzky, M., Turekian, K. K. Spencer, D. W., 1988. Lead-210 and Polonium-210 in ocean water profiles of the continental shelf and slope south of New England. Continental Shelf Research 8, 841–853.

Bacon, M.P., Spencer, D.W., Brewer, P.G., 1976. Pb-210/Ra-226 and Po-210/Pb-210 disequilibria in seawater and suspended particulate matter. Earth and Planetary Science Letters 32, 277–296.

Baskaran, M, 2011. Po-210 and Pb-210 as atmospheric tracers and global atmospheric Pb-210 fallout: a Review. Journal of Environmental Radioactivity, 102, 500-513.

Baskaran, M., Hong, G. H., Santschi , P. H., 2009. Radionuclide analysis in seawater. In: Wurl, O., (Ed.), Practical guidelines for the analysis of seawater. CTC Press, Boca Raton, 259-304.

Baskaran, M., T.M. Church, G.-H. Hong, A. Kumar, M. Qiang, H.-Y. Choi, S. Rigaud, and K. Maiti 2012. Effects of flow rates and composition of the filter, and decay/in-growth correction factors involved with the determination of in-situ particulate ^{210}Po and ^{210}Pb in seawater, Limnol. Oceanogr. (in review).

Bruland, K. W., 1983. Trace elements in seawater. In: Riley, J. P. and Chester, R. (eds.) Chemical Oceanography 8, Academic Press, London, 157-220.

Brewer, P. G., Nozaki, Y., Spencer, D., Fleer, A., 1980. Sediment trap experiments in the deep North Atlantic: isotopic and elemental fluxes. Journal of Marine Research 38,703-728.

Buesseler, K. O., Lamborg, C. H., Boyd, P. W., Lam, P. J., Trull, T. W., Bidigare, R. R., Bishop, J. K. B., Casciotti, K. L., Dehairs, F., Elskens, M., Honda, M., Karl, D. M., Silver, M. W., Steinberg, D. K., Valdes, J., Van Mooy, B., Wilson, S., 2007. Revisiting carbon flux through the ocean's twilight zone. Science 316, 567-570.

Buesseler, K. O., Lamborg, C., Cai, P., Escoube, R., Johnson, R., Pike, S., Masque, P., McGillicuddy, D., Verdeny, E., 2008. Particle fluxes associated with mesoscale eddies in the Sargasso Sea. Deep-Sea Research II 55, 1426-1444.

Chung, Y., Finkel, R., 1988. ^{210}Po in the western Indian Ocean: distributions, disequilibria and partitioning between the dissolved and particulate phases. Earth and Planetary Science Letters 88, 232-240.

Chung, Y., Wu, T., 2005. Large ^{210}Po deficiency in the northern South China Sea. Continental Shelf Research 25, 1209-1224.

Church, T.M. and M.M. Sarin, 2008. U- and The-series nuclides in the atmosphere: Supply, exchange, scavenging and applications to aquatic processes. In: *Radioactivity in the Envi-*

ronment, Vol. 13, Elsevier, p. 11-45.

Church, T.M., S. Rigaud, M. Baskaran, A. Kumar, J. Friedrich, P. Masque, V. Puigcorbe, G. Kim, O. Radakovitch, G. –H. Hong, and G. Stewart, 2012. Inter-calibration studies of ^{210}Po and ^{210}Pb in dissolved and particulate sea water samples. Limnol. Oceanogr. (Methods), accepted for publication.

Cochran, J. K., Bacon, M. P., Krishnaswami, S., Turekian, K. K., 1983.^{210}Po and ^{210}Pb distributions in the central and eastern Indian Ocean. Earth and Planetary Science Letters 65, 433-452.

Cochran, J. K., McKibbin-Vaughan, T., Dornblaser, M. M., Hirschberg, D., Livingston, H. D., Buesseler, K. O., 1990. ^{210}Pb scavenging in the North Atlantic and North Pacific Oceans. Earth and Planetary Science Letters 97, 332-352.

Conte, M. H., Ralph, N., Ross, E. H., 2001. Seasonal and inter-annual variability in deep ocean particle fluxes at the Oceanic Flux Program (OFP)/Bermuda Atlantic Time Series (BATS) site in the western Sargasso Sea near Bermuda. Deep-Sea Research II 48, 1471-1505.

Conte, M. H., Dickey, T. D., Weber, J. C., Johnson, R. J., Knap, A. H., 2003. Transient physical forcing of pulsed export of bioreactive material to the deep Sargasso Sea. Deep-Sea Research I 50, 1157-1187.

Duce, R. A., Liss, P. S., Merrill, J. T., Atlas, E. L., Buat-Menard, P., Hicks, B. B., Miller, J. M., Prospero, J. M, Arimoto, R, Church, T. M., Ellis, W., Galloway, J. N., Jickells, T. D., Knap, A. H., Reinhardt, K. H., Soudine, A., Tokos, J. J., Tsunogai, S., Wollast, R., Zhou, M., 1991. The Atmospheric Input of Trace Species to the World Ocean, Global Biogeochem. Cycles, 5(3), 193-259.

Fisher, N. S., Burns, K. A., Cherry, R. D., Heyraud, M., 1983.Accumulation and cellular distribution of ^{241}Am, ^{210}Po, and ^{210}Pb in two marine algae. Marine Ecology Progress Series 11, 233–237.

Fisher, N. S., Teyssie, J.-L., Krishnaswami, S., Baskaran, M., 1987. Accumulation of Th, Pb, U, and Ra in marine phytoplankton and its geochemical significance. Limnology and Oceanography 32, 131-142.

Harada, K., Tsunogai, S., 1986. Fluxes of ^{234}Th, ^{210}Po and ^{210}Pb determined by sediment trap experiments in pelagic oceans. Journal of Oceanography 42, 192-200.

Hartman, M.C. 1977. The total deposition of Pb, Cd, Zn, ^{210}Pb and atmospheric transport to the western Atlantic using Rn-222 and air mass trajectory analysis, 123 pp., M.S. thesis, Univ. of Del., Newark, 1987.

Heyraud, M., Cherry, R. D., 1979. Polonium-210 and lead-210 in marine food chains. Marine Biology, 52,227-36.

Hong, G. H., Kim, Y. I., Baskaran, M., Kim, S. H., Chung, C. S., 2008. Distribution of ^{210}Po and export of organic carbon from the euphotic zone in the southwestern East Sea (Sea of Japan). Journal of Oceanography 64, 277-292.

Huang, S., Conte, M. H., 2009. Source/process apportionment of major and trace elements in sinking particles in the Sargasso Sea. Geochimica et Cosmochimica Acta 73, 65-90.

Huh, C.-A., Small, L. F., Niemnil, S., Finney, B. P., Hickey, B. M., Kachel, N. B., Gorsline, D. S., Williams, P. M., 1990. Sedimentation dynamics in the Santa Monica-San Pedro Basin off Los Angeles: radiochemical, sediment trap and transmissometer studies. Continental Shelf Research 10, 137-164.

Hussain, N., Church, T. M., Larson, R. E., 1998. Radon daughter disequilibria and lead systematics in the western North Atlantic. Journal of Geophysical Research, 103, 16059-16071.

Kadko, D., 1983. Excess ^{210}Po and nutrient recycling within the California coastal transition zone. Journal of Geophysical Research 98, 857-864.

Kharkar, D. P., Thomson, J., Turekian, K. K., Foster, W.O., 1976. Uranium and thorium decay series nuclides in plankton from the Caribbean. Limnology and Oceanography 21, 294-299.

Kim, G., Alleman, L. Y., Church, T. M., 1999. Atmospheric depositional fluxes of trace elements, ^{210}Pb, and ^{7}Be to the Sargasso Sea. Global Biogeochemical Cycles 13, 1183-1192.

Kim, G., 2001. Large deficiency of polonium in the oligotrophic ocean's interior. Earth and Planetary Science Letters 192, 15-21.

Kim, G., Church, T. M., 2001. Seasonal biogeochemical fluxes of ^{234}Th and ^{210}Po in the upper Sargasso Sea: Influence from atmospheric iron deposition. Global Biogeochemical Cycles 15, 651-661.

Masqué, P., Sanchez-Cabeza, J. A., Bruach, J. M., Palacios, E., Canals, M., 2002. Balance and residence times of ^{210}Pb and ^{210}Po in surface waters of the northwestern Mediterranean Sea. Continental Shelf Research 22, 2127-2146.

McCave, I. N., Hall, I. R., Anita, A. N., Chou, L., Dehairs, F., Lampitt, R. S., Thomsen, L., Van Weering, T. C. E., Wollast, R., 2001. Distribution, composition and flux of particulate material over the European margin at 47–50^{o}N.Deep Sea Research II 48, 3107–3139.

McNeary, D. Baskaran, M. 2007. Residence times and temporal variations of ^{210}Po in aerosols and precipitation from southeastern Michigan, United States. Journal of Geophysical Research 112, 11 pages, D04208, doi:10.1029/2006JD007639.

Moore, W. S., Bruland, K. W., Michel, J., 1981. Fluxes of uranium and thorium series isotopes in the Santa Barbara Basin. Earth and Planetary Science Letters 53, 391-399.

Nozaki, Y., Thomson, J., Turekian, K.K., 1976. The distribution of Pb-210 and Po-210 in the surface waters of the Pacific Ocean. Earth and Planetary Science Letters 32,304–312.

Nozaki, Y., Zhang, J., Takeda, A., 1997. ^{210}Pb and ^{210}Po in the equatorial Pacific and the Bering Sea: the effects of biological productivity and boundary scavenging. Deep-Sea Research II 44, 2203-2220.

Nozaki, Y., Tsunogai, S., 1976. ^{226}Ra, ^{210}Pb and ^{210}Po disequilibria in the Western North Pacific Ocean. Earth and Planetary Science Letters 32, 313-321.

Nozaki, Y., Naoko, I., Yashima, M., 1990. Unusually large ^{210}Po deficiencies relative to ^{210}Pb in the Koroshio Current of the East China and Philippine Seas, Journal of Geophysical Research 95, 5321-5329.

Nozaki, Y., Tsubota, H., Kasemsupaya, V., Yashima, M., Ikura, N., 1991. Residence times of surface water and particle-reactive ^{210}Pb and ^{210}Po in the East China and Yellow Seas. Geochimica et Cosmochimica Acta 55, 1265-1274.

Prospero, J.M., 1996. Saharan dust transport over the North Atlantic Ocean and Mediterranean: An overview, *The impacts of Desert Dust Across the Mediterranean*, edited by S. Guerzoni and R. Chester, 133-151.

Sarin, M.M., Krishnaswami, S., Ramesh, R., Somayajulu, B.L.K., 1994. ^{238}U decay series nuclides in the northeastern Arabian Sea: Scavenging rates and cycling processes. Cont. Shelf Res., 14: 251-265.

Sarin, M. M., Kim, G., Church, T. M., 1999. Po-210 and Pb-210 in the South-equatorial Atlantic: distribution and disequilibrium in the upper 500 m. Deep-Sea Research II 46, 907-917.

Settle, D. M., Patterson, C. C., Turekian, K. K., Cochran, J. K., 1982: Lead precipitation fluxes at tropical oceanic sites determined from ^{210}Pb measurements, Journal of Geophysical Research87, 1239–1245.

Shannon, L. V., Cherry, R. D., Orren, M. J., 1970. Polonium-210 and Lead-210 in the marine environment. Geochim. Cosmochim. Acta 34, 701-711.

Stewart, G. M., Fowler, S. W., Teyssie, J. L., Cotret, O., Cochran, J. K., Fisher, N. S., 2005. Contrasting transfer of polonium-210 and lead-210 across three trophic levels in marine plankton. Marine Ecology-Progress Series 290, 27-33.

Stewart, G. M., Moran, S. B., Lomas, M. W., 2010. Seasonal POC fluxes at BATS estimated from ^{210}Po deficits. Deep-Sea Research I 157, 113-124.

Taylor, S. R., McLennan, S. M., 1985. The Continental Crust: Its Composition and Evolution. Blackwell Scientific, Oxford. 328p.

Thomson, J., Turekian, K.K., 1976. Polonium-210 and Lead-210 distributions in ocean water

profiles from the eastern South Pacific. Earth Planet. Sci. Lett. 32, 297–303.

Tsunogai, S., Nozaki, Y., 1971. Lead-210 and polonium-210 in surface water of the Pacific. Geochemical Journal 5, 165-173**.**

Turekian, K. K., Benninger, L. K., Dion, E. P., 1983. ^{7}Be and ^{210}Pb total deposition fluxes at New Haven, Connecticut and at Bermuda. Journal of Geophysical Research 88, 5411-5415.

Turekian, K. K., Nozaki, Y., 1980. ^{210}Po and ^{210}Pb in the Eastern South Pacific- the role of upwelling on their distributions in the water column. In: Goldberg, E. D., Horibe, Y., Saruhashi, K. (eds.) Isotope Marine Chemistry, Uchida Rokakuho Publ. Co. Tokyo.p. 157-164.

Veron, A. J., Church, T. M., Flegel, R., Patterson, C. C., Erel, Y., 1993. Response of lead cycling in the surface Sargasso Sea to changes in tropospheric input. Journal of Geophysical Research 98, C10, 18269-18276.

636 Table 1. Inventories* (dpm m^{-2}) of filtered (f) and unfiltered (uf) ^{210}Po and ^{210}Pb, particulate
637 ^{210}Po ($^{210}Po_p$) and ^{210P}b ($^{210}Pb_p$) and $^{210}Po/^{210}Pb$ activity ratios in the upper 500 meter water
638 column

Date	$^{210}Po_f$ Inventory	$^{210}Po_{uf}$ Inventory	$^{210}Pb_f$ Inventory	$^{210}Pb_{uf}$ Inventory	$(^{210}Po/^{210}Pb)_f$ Activity ratio	$^{210}Po_p$ (%)	$^{210}Pb_p$ (%)	POC (mol m^{-2})
Sept. 1999	36236	51257	NM	NM	-	29	-	0.94
Dec. 1999	44818	60889	NM	NM	-	26	-	0.64
Jan. 2000	29898	39566	79945	85287	0.37±0.01	24	6	0.55
March 2000	30310	45846	83305	90239	0.36±0.01	34	8	-
May 2000	24391	31092	81575	93272	0.30±0.01	22	13	-
Sept. 2000	27729	38819	106427	135924	0.26±0.01	29	22	0.91

639 *: The propagated error on the inventories is less than 5%
640
641

642 Table 2. Average chemical composition of settling particles for the period May 1999-May
643 2000.
644

Depth (m)	Mass flux mg m^{-2} d^{-1}	Lithogenic material (%)	Biogenic material			^{210}Po (dpm/mg)	^{210}Pb (dpm/mg)
			Organic matter (%)	$CaCO_3$ (%)	Opal (%)		
500	25.8±19.9 (N=24)	5.5± 4.7 (N=24)	29.7± 15.2 (N=24)	46.9± 18.6 (N=24)	19.9± 22.5 (N=24)	0.27± 0.18 (N=20)	0.54± 0.40 (N=15)
1500	41.2± 15.3 (N=24)	12.5± 5.0 (N=24)	15.4± 3.8 (N=24)	61.3± 6.7 (N=24)	10.8± 7.9 (N=24)	0.28± 0.10 (N=15)	0.38± 0.33 (N=13)
3200	41.7± 20.9 (N=24)	18.8 ±9.0 (N=24)	11.2 ± 1.5 (N=24)	57.6± 5.3 (N=24)	12.3± 7.6 (N=24)	0.40± 0.19 (N=15)	1.02± 0.42 (N=10)

645 N= number of samples.
646
647
648

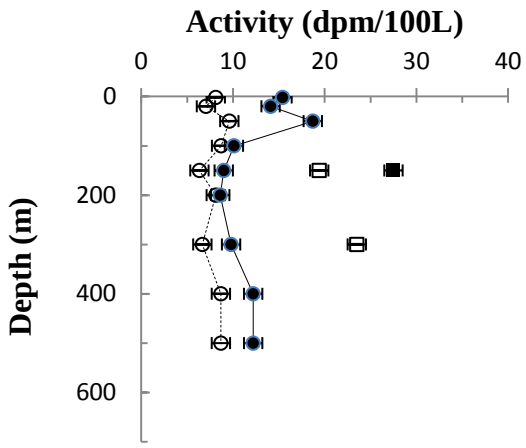

(A) September 1999

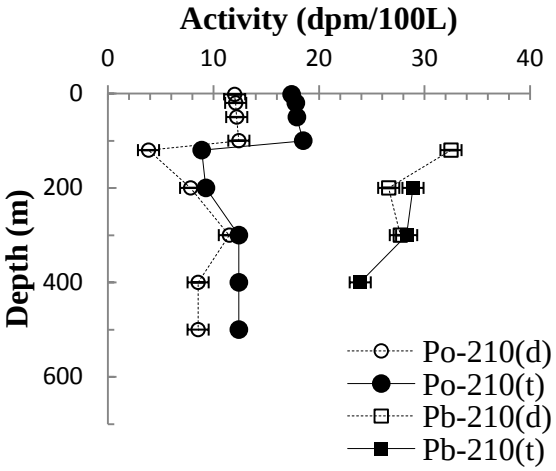

(B) December 1999

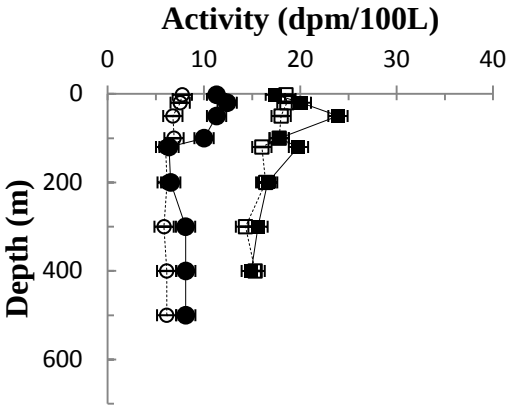

(C) January 1999

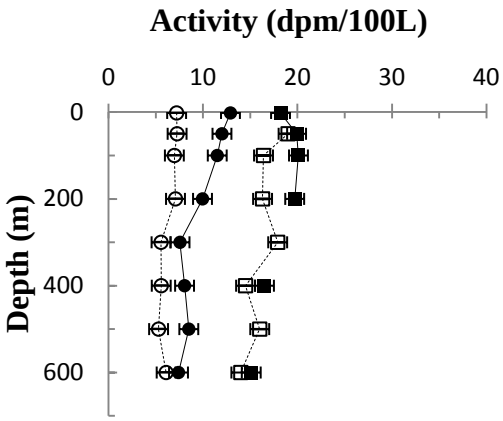

(D) March 2000

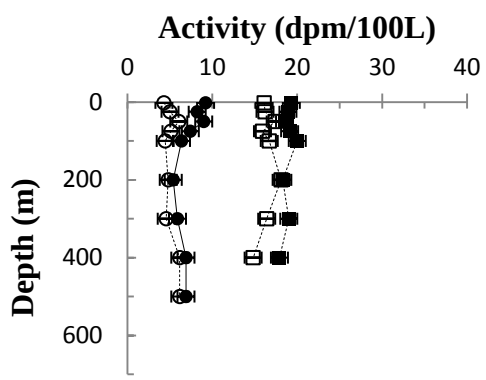

(E) May 2000

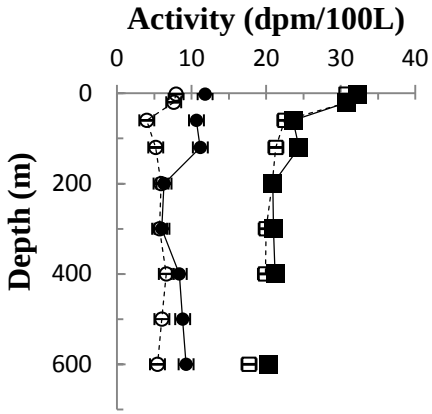

(F) September 2000

649 Figure 1. Vertical Profiles of activities of ^{210}Po and ^{210}Pb in the water column. The counting errors
650 were less than 10% and are not included in the size of the symbol.
651
652
653

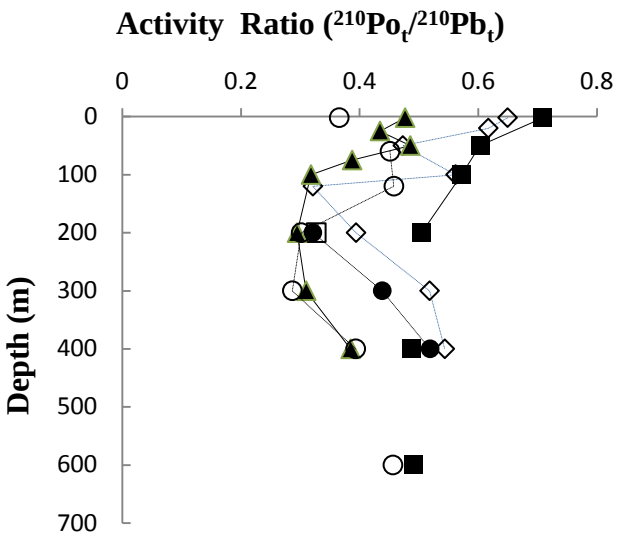

(a)

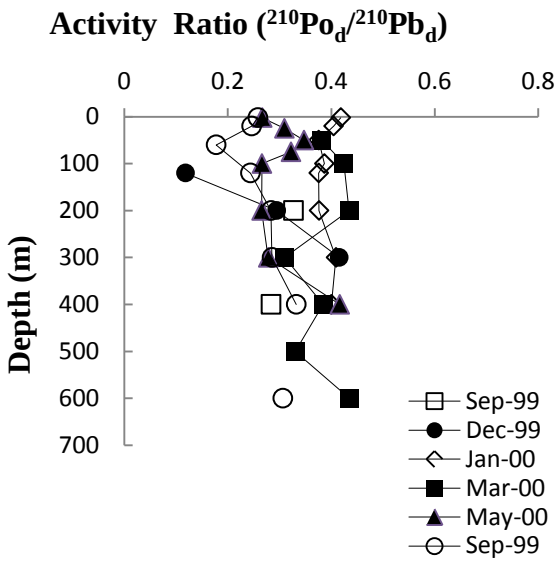

(b)

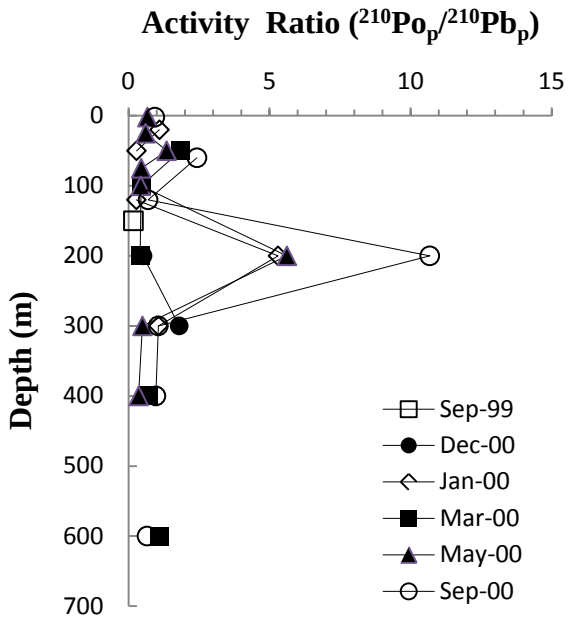

(c)

Figure 2. Activity ratios of $^{210}Po/^{210}Pb$ in the total (a), dissolved (b), and particulate phases(c) in the water column. The subscripts of t, d, and p denote total, dissolved and particulate phases of both ^{210}Po and ^{210}Pb, respectively. The counting errors were less than 10% and are not included in the size of the symbol.

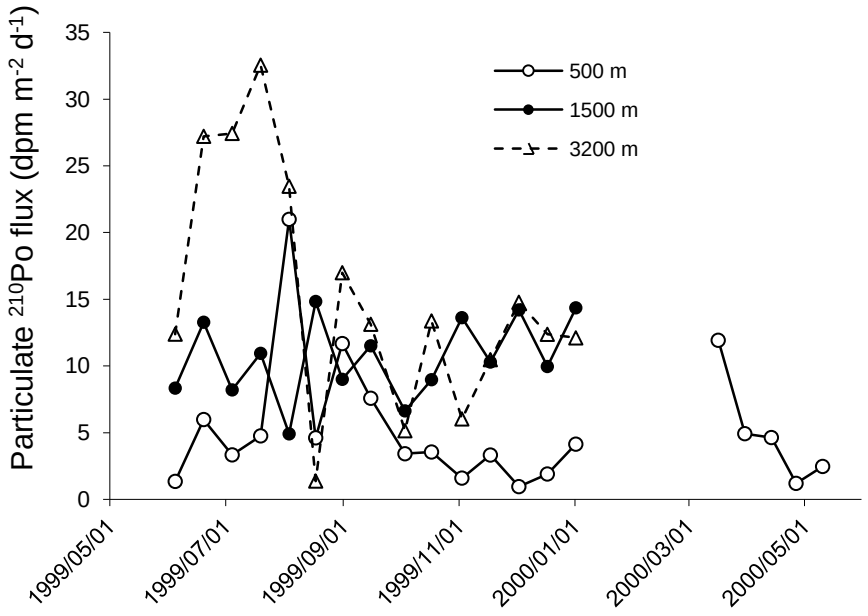
Particulate ^{210}Po flux (dpm m^{-2} d^{-1})
35
30
25
20
15
10
5
0
500 m
1500 m
3200 m
1999/05/01
1999/07/01
1999/09/01
1999/11/01
2000/01/01
2000/03/01
2000/05/01

(a)

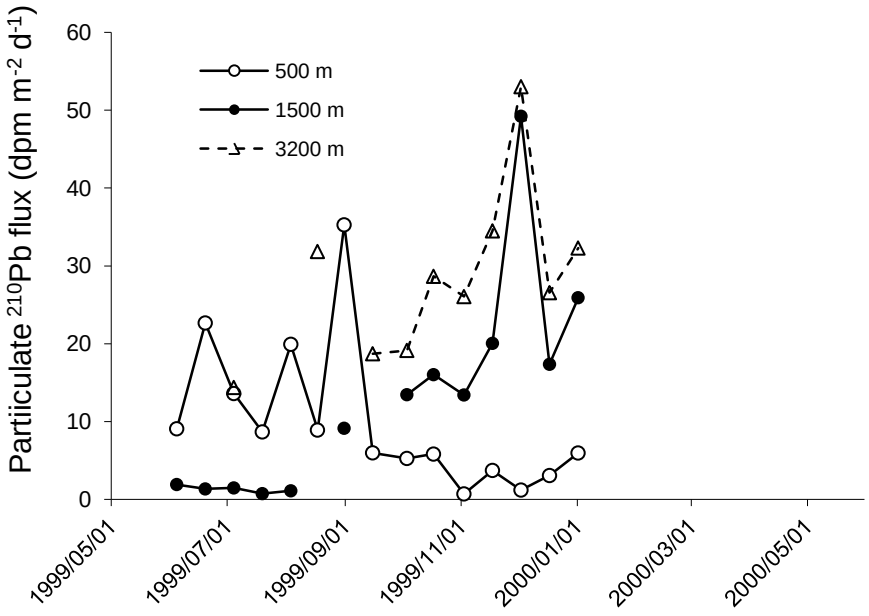
Partiiculate ^{210}Pb flux (dpm m^{-2} d^{-1})
60
50
40
30
20
10
0
500 m
1500 m
3200 m
1999/05/01
1999/07/01
1999/09/01
1999/11/01
2000/01/01
2000/03/01
2000/05/01

(b)

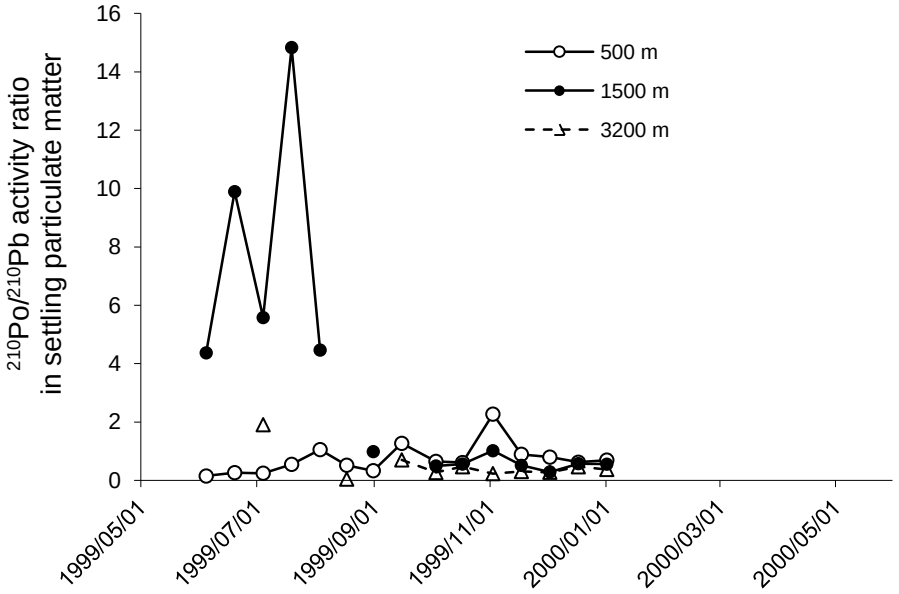

(c)

Figure 3. Temporal variation of settling fluxes of particulate ^{210}Pb (a), ^{210}Po (b), and their activity ratio (^{210}Po/^{210}Pb) in sediment traps at 500, 1500, and 3200 m depths from May 1999-May 2000. X-axis is date expressed as yyyy-mm-dd.

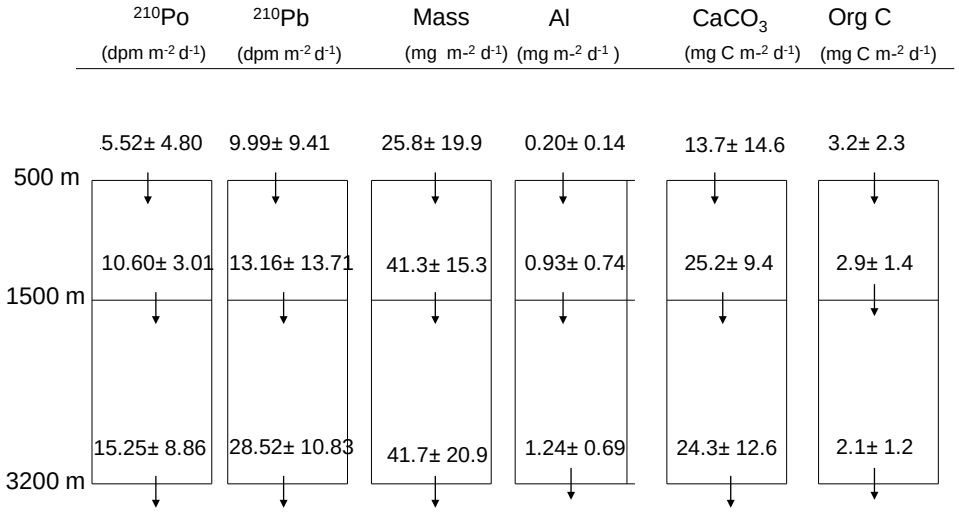

Figure 4. Average settling fluxes of particulate ^{210}Po, ^{210}Pb,bulk mass, Al, $CaCO_3$ and organic carbon at 500, 1500, and 3200 m depths from May 1999 to May 2000.

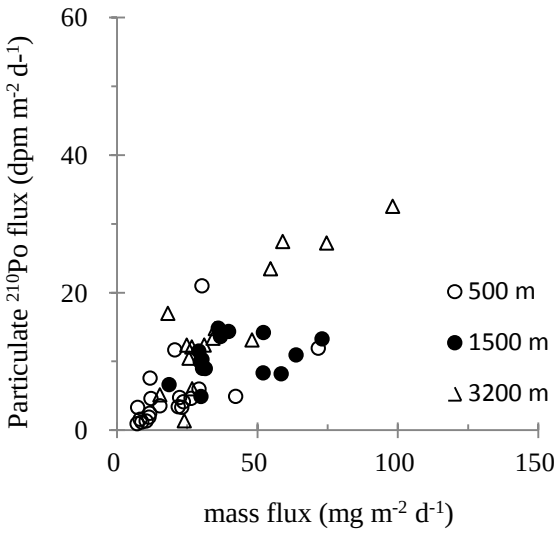
Particulate ^{210}Po flux (dpm m^{-2} d^{-1})
60
40
20
0
0
50
100
150
mass flux (mg m^{-2} d^{-1})
500 m
1500 m
3200 m

(a)

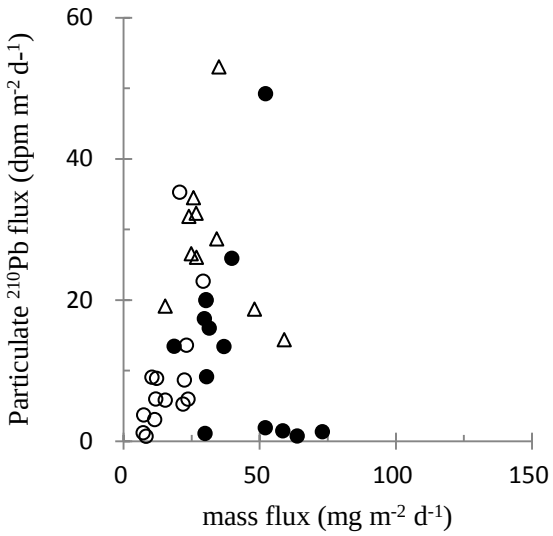
Particulate ^{210}Pb flux (dpm m^{-2} d^{-1})
60
40
20
0
0
50
100
150
mass flux (mg m^{-2} d^{-1})

(b)

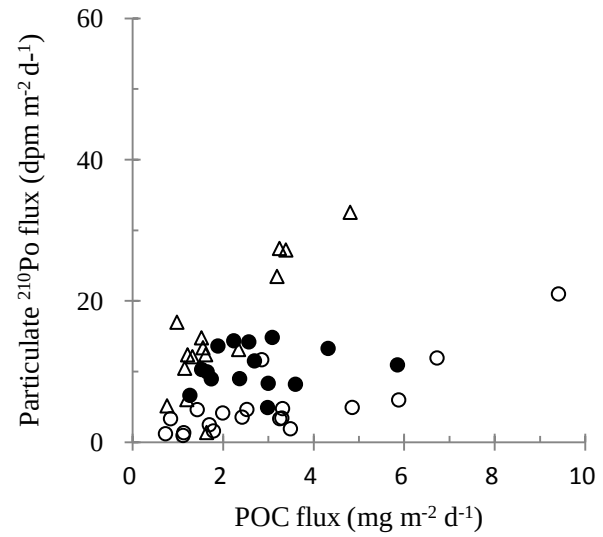
Particulate ^{210}Po flux (dpm m^{-2} d^{-1})
POC flux (mg m^{-2} d^{-1})
0
20
40
60
0
2
4
6
8
10

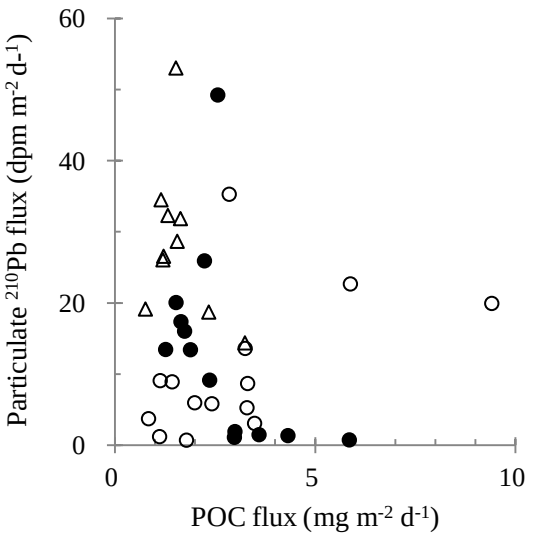
Particulate ^{210}Pb flux (dpm m^{-2} d^{-1})
POC flux (mg m^{-2} d^{-1})
0
20
40
60
0
5
10

(c)

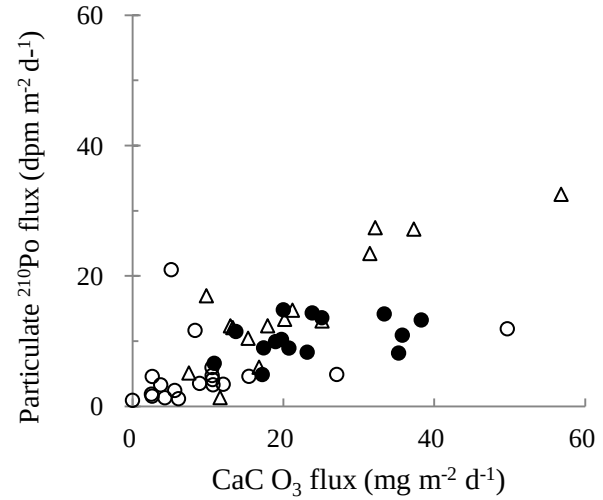
Particulate ^{210}Po flux (dpm m^{-2} d^{-1})
CaC O_3 flux (mg m^{-2} d^{-1})
0
20
40
60
0
20
40
60

(d)

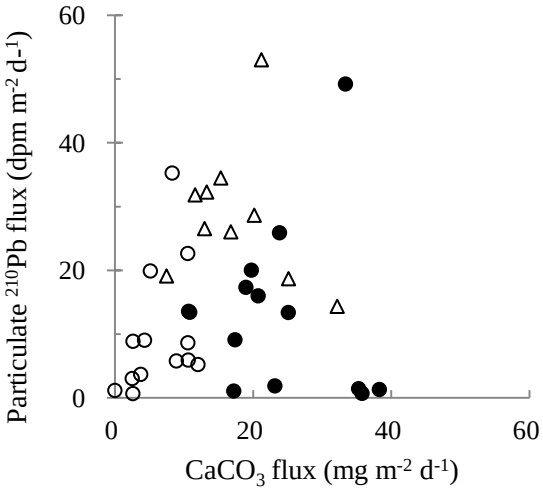
Particulate ^{210}Pb flux (dpm m^{-2} d^{-1})
$CaCO_3$ flux (mg m^{-2} d^{-1})
0
20
40
60
0
20
40
60

(e)

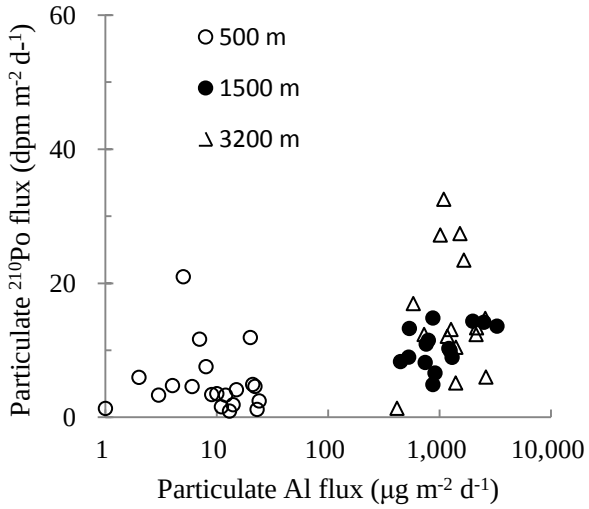
60
40
20
0
500 m
1500 m
3200 m
Particulate ^{210}Po flux (dpm m^{-2} d^{-1})
1
10
100
1,000
10,000
Particulate Al flux (µg m^{-2} d^{-1})

(f)

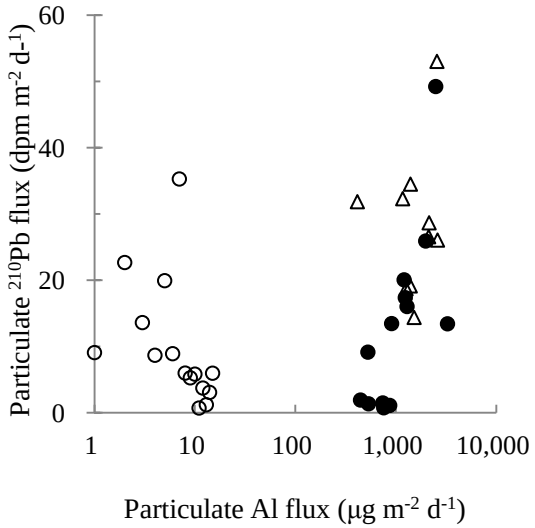
60
40
20
0
Particulate ^{210}Pb flux (dpm m^{-2} d^{-1})
1
10
100
1,000
10,000
Particulate Al flux (µg m^{-2} d^{-1})

(g)

(h)

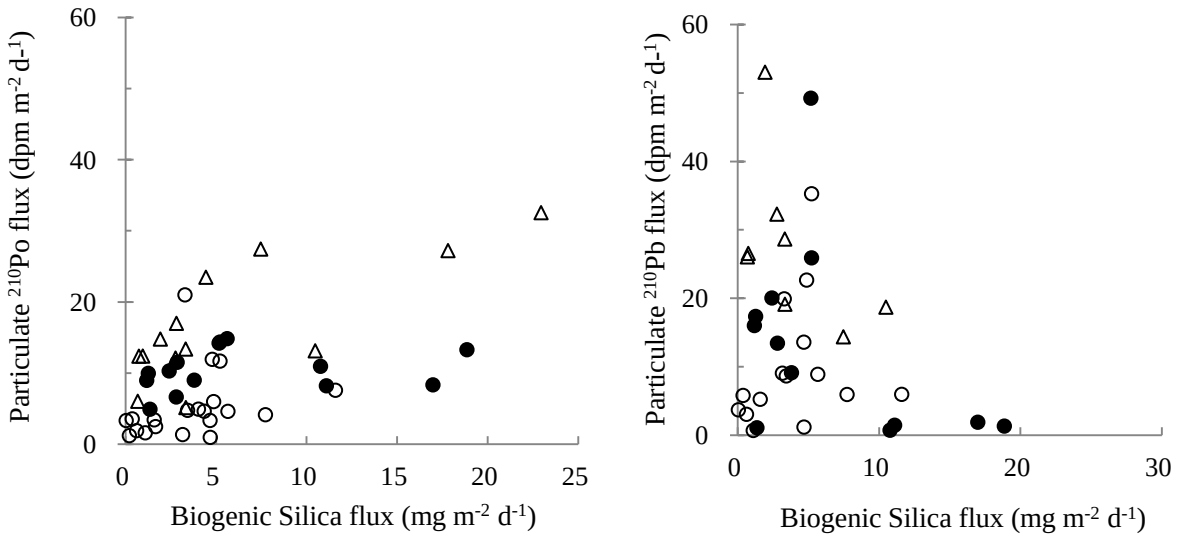

Figure 5. Association of particulate ^{210}Po and ^{210}Pb to the major carrier phases of the settling particulate matter, bulk mass (a, b), particulate organic carbon (POC) (c,d), and calcium carbonate ($CaCO_3$) (e, f), particulate Al (g, h), and biogenic silica fluxes (i, j) for the entire depth samples.

Appendix-I: Concentrations of POC, filtered (f) and unfiltered (uf) ^{210}Po and ^{210}Pb and percentages of particulate* ^{210}Po and ^{210}Pb in the upper 600m

Depth (m)	POC (μ M)	$^{210}Po_f$ (dpm/100L)	$^{210}Po_{uf}$ (dpm/100L)	$^{210}Po_p$ (%)	$^{210}Pb_f$ (dpm/100L)	$^{210}Pb_{uf}$ (dpm/100L)	$^{210}Pb_p$ (%)
September	1999-16						
2	2.58	8.12±0.34	15.4±0.6	47.2	NM	NM	-
20	2.62	7.05±0.32	14.1±0.6	50.1	NM	NM	-
50	2.50	9.60±0.40	18.7±0.7	48.6	NM	NM	-
100	NM	8.70±0.39	10.1±0.5	14.2	NM	NM	-
150	2.21	6.34±0.26	8.99±0.35	29.5	19.4±0.9	27.5±1.3	29.4
200	1.82	8.12±0.37	8.61±0.37	5.7	NM	NM	-
300	1.38	6.66±0.25	9.79±0.37	32.0	23.5±1.1	22.1±1.3	-
400	1.48	8.68±0.35	12.2±0.5	28.8	NM	NM	-
December	1999-17						
2	2.16	12.0±0.4	17.4±0.7	31.0	NM	NM	-
20	2.00	12.1±0.4	17.8±0.6	32.3	NM	NM	-
50	2.19	12.2±0.4	17.9±0.7	31.7	NM	NM	-
100	NM	12.4±0.5	18.5±0.7	32.7	NM	NM	-
120	NM	3.84±0.16	8.88±0.48	56.7	32.5±1.7	NM	-
200	0.90	7.83±0.39	9.28±0.46	15.6	26.6±1.3	28.9±1.6	7.9
300	1.00(m)	11.5±0.6	12.4±0.6	6.9	27.7±1.5	28.3±1.2	2.2
400	1.09	8.54±0.38	12.4±0.7	30.8	-	23.9±1.1	-
January	2000-18						
2	2.08	7.74±0.50	11.3±0.5	31.4	18.5±1.0	17.4±0.8	-6.4
20	2.48	7.52±0.44	12.4±0.6	39.6	18.6±0.8	20.1±0.9	7.5

50	2.23	6.76±0.39	11.3±0.0.6	40.3	18.0±0.7	23.9±1.2	24.7
100	NM	6.88±0.46	10.0±00.4	31.3	17.8±0.7	17.8±0.8	-0.1
120	NM	6.01±0.37	6.36±0.36	5.6	16.0±0.7	19.8±0.8	19.0
200	0.67	6.17±0.31	6.54±0.30	5.6	16.4±0.9	16.6±0.8	1.2
300	0.76	5.85±0.42	8.08±0.35	27.6	14.3±0.6	15.6±0.7	8.0
400	0.73	6.12±0.34	8.10±0.38	24.4	15.3±0.7	14.9±0.6	-2.5
March	2000-19						
2	1.91	7.20±0.38	12.9±0.6	44.3	-	18.2±0.8	-
50	NM	7.25±0.55	12.0±0.5	39.4	19.0±0.9	19.9±0.9	4.5
100	NM	6.96±0.39	11.5±0.6	39.4	16.4±0.7	20.1±0.8	18.2
200	NM	7.08±0.34	9.94±0.49	28.8	16.3±0.7	19.7±1.1	17.4
300	NM	5.55±0.34	7.56±0.46	26.6	17.9±0.9	16.8±1.0	-6.4
400	NM	5.57±0.28	8.04±0.56	30.7	14.5±0.6	16.5±0.8	11.9
500	NM	5.29±0.29	8.49±0.50	37.7	16.0±0.7	15.3±0.6	-5.0
600	NM	6.09±0.50	7.40±0.56	17.7	14.0±0.5	15.1±0.6	7.3
May	2000-20						
2	2.22	4.29±0.20	9.20±0.35	53	16.1±0.8	19.3±0.8	16.5
25	2.18	5.01±0.26	8.21±0.45	39	16.2±0.6	18.9±0.7	14.4
50	4.10	6.04±0.25	8.98±0.35	33	17.4±0.7	18.5±0.8	6.0
75	NM	5.12±0.24	7.40±0.32	31	15.9±0.7	19.1±0.8	16.5
100	NM	4.44±0.20	6.36±0.25	30	16.7±0.7	20.0±0.7	16.5
200	1.56	4.80±0.22	5.39±0.23	11	18.1±0.7	18.3±0.7	1.1
300	1.01	4.56±0.18	5.89±0.23	23	16.4±0.6	19.0±0.7	13.7
400	1.20	6.16±0.26	6.89±0.27	11	14.8±0.7	17.9±0.7	17.4
September	2000–21						

2	NM	7.92±0.37	11.81±0.49	33	30.7±1.2	32.3±1.3	4.8
20	NM	7.60±0.37	5.08±0.26	-	30.9±1.2	30.8±1.2	-
60	NM	3.99±0.17	10.65±0.40	63	22.5±0.8	23.6±0.9	4.7
120	NM	5.19±0.25	11.17±0.45	54	21.3±0.8	24.4±1.1	12.6
200	NM	5.90±0.24	6.30±0.25	6.3	20.8±1.1	20.9±0.9	0.8
300	NM	5.71±0.26	6.02±0.26	5.1	20.0±0.8	21.0±1.0	5.0
400	NM	6.61±0.27	8.34±0.34	21	19.9±1.0	21.2±0.9	6.2
600	NM	5.42±0.26	9.26±0.45	42	17.7±0.8	20.3±0.9	12.6

***:** particulate ^{210}Po or ^{210}Pb activity = (unfiltered – filtered) activity of ^{210}Po or ^{210}Pb

Appendix-II: Settling fluxes of ^{210}Po and ^{210}Pb, Al, organic carbon and carbonate.

Depth	500 m							
Trap sampling dates (mm/dd/yy)	Flux ($m^{-2}d^{-1}$) Mass (mg)	Al (μg)	Org C (mg	$CaCO_3$ (mg)	^{210}Po (dpm)		^{210}Pb (dpm)	
5/28- 6/12 1999	10.40	38	1.13	4.3	1.35	± 0.007	9.07	± 0.06
6/12- 271999	29.21	73	5.88	10.5	5.98	± 0.009	22.7	± 0.1
6/27- 7/121999	23.07	48	3.25	10.7	3.33	± 0.008	13.6	± 0.1
7/12- 271999	22.31	87	3.31	10.6	4.76	± 0.014	8.67	± 0.03
7/27- 8/101999^{+}	30.26	96	9.41	Nd	21.0	± 0.05	19.9	± 0.1
8/10- 241999	12.11	57	1.43	2.62	4.61	± 0.01	8.91	± 0.05
8/24- 9/8/1999	20.59	67	2.85	8.29	11.68	± 0.02	35.3	± 0.2
9/8- 231999^{+}	11.79	16	Nd	Nd	7.58	± 0.02	5.98	± 0.03
9/26- 10/101999	23.37	80	3.53	12.9	3.42	± 0.01	5.26	± 0.02
10/10- 25199	15.28	58	2.42	8.90	3.55	± 0.01	5.82	± 0.03
10/25- 11/101999	8.24	52	1.79	2.60	1.59	± 0.01	0.70	± 0.02
11/10- 251999	7.36	146	0.84	3.74	3.32	± 0.01	3.72	± 0.06
11/25- 12/101999^{+}	7.17	2	1.12	Nd	0.95	± 0.01	1.20	± 0.03
12/10- 251999^{+}	11.39	50	3.49	Nd	1.90	± 0.01	3.06	± 0.03
12/25/1999	23.65	77	1.99	10.6	4.14	± 0.01	5.96	± 0.02

-1/8/2000								
1/10-25					ND		ND	
2000	18.56	180	1.55	11.0				
1/25-					ND		ND	
2/92000	54.37	194	5.09	36.3				
2/9-232000	73.50	279	6.36	45.7	ND		ND	
2/23-					ND		ND	
3/92000	57.89	432	5.21	39.4				
3/9-23							ND	
2000	71.68	202	6.73	49.7	11.9	0.1		
3/23-4/6							ND	
2000	42.26	40	4.85	27.1	4.92	0.01		
4/6-202000	26.37	87	2.53	15.4	4.63	0.02	ND	
4/20-							ND	
5/32000	8.83	77	0.73	6.10	1.20	0.02		
5/3-172000	11.67	57	1.70	5.60	2.47	0.03	ND	
		1500 m						
5/28- 6/12								
1999	52.04	446	3.00	23.2	8.34	± 0.21	1.91	± 0.09
6/12-								
271999	73.02	536	4.32	38.3	13.3	± 0.4	1.34	± 0.05
6/27-								
7/121999	58.47	351	3.60	35.3	8.20	± 0.22	1.47	± 0.06
7/12-								
271999	63.77	366	5.85	35.8	11.0	± 0.3	0.74	± 0.04
7/27-								
8/101999	29.90	402	2.98	17.2	4.91	± 0.17	1.10	± 0.04
8/10-								
241999	36.07	309	3.09	20.0	14.8	± 0.2	ND	
8/24-								
9/8/1999	30.47	343	2.37	17.4	9.00	± 0.13	9.14	± 0.53
9/8-231999	29.14	559	2.69	13.7	11.5	± 0.15		

9/26-10/101999	18.55	179	1.27	10.8	6.63	±	0.07	13.5	± 0.1
10/10-25199	31.45	480	1.74	20.7	8.97	±	0.17	16.0	± 0.1
10/25-11/101999	36.85	755	1.89	25.1	13.6	±	0.2	13.4	± 0.1
11/10-251999	30.27	398	1.53	19.8	10.3	±	0.1	20.1	± 0.1
11/25-12/101999	52.14	667	2.57	33.4	14.2	±	0.2	49.2	± 1.9
12/10-251999	29.66	488	1.65	19.0	9.96	±	0.15	17.4	± 1.1
12/25/1999-1/8/2000	39.74	485	2.24	23.8	14.4	±	0.2	25.9	± 1.2
1/10-25 2000	15.01	167	0.97	9.58	ND			ND	
1/25-2/92000	33.18	338	2.61	21.1	ND			ND	
2/9-232000	59.58	391	4.71	37.9	ND			ND	
2/23-3/92000	58.64	386	5.91	40.8	ND			ND	
3/9-23 2000	54.46	301	5.61	36.5	ND			ND	
3/23-4/6 2000	57.93	312	3.48	38.1	ND			ND	
4/6-202000	36.75	289	2.35	24.3	ND			ND	
4/20-5/32000	31.81	312	1.90	21.6	ND			ND	
5/3-172000	32.79	320	1.77	22.5	ND			ND	
5/28- 6/12	31.08	727	1.62	17.9	12.4	±	0.2	ND	

(mm/dd/yy)	Mass (mg)	Al (μg)	Org C (mg C)	3200 m $CaCO_3$ (mg)	^{210}Po (dpm)	^{210}Pb (dpm)

1999										
6/12-271999	74.65	1015	3.39	37.3	27.2	±	0.5	ND		
6/27-7/121999	59.01	1027	3.25	32.2	27.4	±	0.4	14.4	±	1.0
7/12-271999	98.17	657	4.81	56.8	32.6	±	0.5	ND		
7/27-8/101999	54.68	987	3.19	31.5	23.5	±	0.3	ND		
8/10-241999	23.97	776	1.64	11.6	1.37	±	0.04	31.9	±	1.6
8/24-9/8/1999	18.12	282	0.98	9.8	17.0	±	0.2	ND		
9/8-231999	48.08	614	2.34	25.1	13.1	±	0.2	18.7	±	0.6
9/26-10/101999	15.28	234	0.76	7.5	5.15	±	0.11	19.1	±	1.0
10/10-25199	34.20	611	1.56	20.2	13.4	±	0.3	28.7	±	1.1
10/25-11/101999	26.76	560	1.20	16.8	6.03	±	0.07	26.1	±	1.1
11/10-251999	25.66	705	1.15	15.3	10.5	±	0.2	34.5	±	1.4
11/25-12/101999	35.01	716	1.52	21.2	14.8	±	0.1	53.0	±	2.2
12/10-251999	24.84	709	1.22	13.0	12.4	±	0.1	26.6	±	1.3
12/25/1999-1/8/2000	26.64	645	1.32	13.3	12.1	±	0.1	32.3	±	1.4
1/10-25 2000	15.47	260	0.88	8.52	ND			ND		
1/25-2/92000	29.20	277	1.59	17.6	ND			ND		
2/9-232000	71.40	447	4.66	44.6	ND			ND		
2/23-	46.28	379	2.39	29.6	ND			ND		

3/92000						
3/9-23					ND	ND
2000	59.92	437	3.45	38.4		
3/23-4/6					ND	ND
2000	61.15	425	3.29	39.7		
4/6-202000	44.15	327	1.90	28.2	ND	ND
4/20-					ND	ND
5/32000	37.93	398	1.60	22.8		
5/3-172000	39.90	442	1.70	25.3	ND	ND

ND: no data

+: Samples that had a few fish fragments.